Environ. Sci. Technol. **2005**, *39,* 6306−6312

Field Column Study Using Zerovalent Iron for Mercury Removal from Contaminated Groundwater

CHRISTOPHER G. WEISENER,*,†
K. SCOTT SALE,
DAVID J. A. SMYTH, AND
DAVID W. BLOWES

Department of Earth Sciences, University of Waterloo, Waterloo, Ontario, Canada N2L 3G1

Passive in situ remediation technologies, for example, permeable reactive barriers, PRBs, are an attractive and less expensive alternative compared to conventional pump and treat systems for groundwater remediation. Field column experiments were conducted to evaluate the removal of dissolved mercury from groundwater using zerovalent iron as the reactive media. Two column tests were conducted over a 6-week period, which simulated 2 and 10 years of groundwater flow through a potential full-scale treatment system. The influent groundwater pH was 7.8−9.5. The groundwater was reduced with an Eh, corrected to the standard hydrogen electrode, ranging from 0 to 120 mV over the trial period. Prior to treatment the total mercury concentration of the groundwater was approximately 40 μg L^{-1}. Effluent from the 10-year simulation contained approximately 0.5 μg/L of mercury during the first 3 weeks and increased to as much as 4 μg L^{-1} by the end of the testing period. Effluent from the 2-year simulation was generally <0.1 μg L^{-1}. Profile sampling of the 2-year simulation suggests that most of the mercury removal occurred in the initial 50% of the 20 cm column. Mineralogical studies, conducted using SEM/EDS and X-ray absorption spectroscopy (XAS), confirm the accumulation of mercury onto a zerovalent iron surface in this 20-cm zone. These analyses indicate that mercury accumulated as a mercury sulfide with a stoichiometery similar to those of cinnabar and metacinnabar (HgS).

Introduction

Mercury (Hg) is a well-known environmental pollutant because of its toxicity and its ability to bioaccumulate in the food chain. The toxicological concern to both fish and wildlife is undisputed and human health concerns arise in the vicinity of Hg-contaminated sites (*1*). Mercury can enter the environment from several sources including material processing, waste disposal, mining and smelting activities, chloralkali plants associated with pulp and paper production, and natural sources (*2*−*8*). The remediation of Hg from contaminated groundwater is important both to industry and to government agencies monitoring mine closures and cleanup activities at industrial sites. Permeable reactive barriers (PRBs) show promise for the passive in situ interception and removal of dissolved inorganic contaminants, such as Hg, from contaminated groundwater. The PRB technology has proven to be a low-cost alternative to traditional treatment methods (*9*−*17*). Permeable reactive barriers are installed in the path of migrating groundwater that contains organic and/or inorganic contaminants. These barriers are composed of reactive solids that remove contaminants by reactions that occur within the barrier. The reduction of H_2O by Fe(0) releases $H_{2(g)}$, which may be used by sulfate-reducing bacteria as an electron donor. Sulfate reduction may result in subsequent precipitation of sparingly soluble metal-sulfide solids (*10*, *18*).

In this study we used field-based column experiments in conjunction with synchrotron analyses of the solid-phase column materials to assess the potential for removal of Hg from contaminated groundwater. The flow rate through the columns was set to simulate the equivalent volume of 2 and 10 years of groundwater flow. X-ray adsorption spectroscopy (i.e., micro X-ray radiation fluorescence (μ-SXRF) and micro extended X-ray adsorption fine structure (μ-EXAFS)) and SEM were used to examine the column materials to identify the accumulation of reaction products. The synchrotron technique is an element-specific, nondestructive method which provides detailed information on the local chemical environment and valence state of elements (*4*, *20*−*23*).

Methods

Column Design and Field Conditions. Field testing, using two columns containing zerovalent iron, was conducted to assess the potential for removal of mercury from groundwater at an industrial site in the eastern United States. A schematic diagram illustrating the configuration of a treatment column is shown in Figure 1. The columns were constructed at the University of Waterloo from acrylic material. The overall internal column length was 21.7 cm and the internal diameter was 5 cm. The internal volume of each column was 425 mL. The columns were packed with zerovalent iron; no other reactive material was used. The reactive material was placed within a zone approximately 18.4 cm in length in each column and was bounded by sand layers approximately 1.8 and 1.6 cm in thickness at the base and the top of each column, respectively. The zerovalent iron is available commercially (iron aggregate ETI−CC-1004; Connelly-GPM, Inc., Chicago). The iron ranged in grain size from less than U.S. Standard Mesh 8 (2.38-mm grain diameter) to in excess of Standard Mesh 50 (0.3-mm grain diameter) and was similar in character to a medium-coarse sand. Sampling ports constructed of 0.32-cm diameter threaded nylon connectors were installed at 2.5-cm intervals along the length of each column.

The low flow-rate column (column A) contained 96 g of sand within the sand filter layers. Column A contained 1085 g of zerovalent iron. Column A had a dry weight of 2319 g and a wet weight of 2554 g. The pore volume for column A was 210.3 mL. The high flow-rate column (column B) contained 93 g of silica sand and 1067 g of zerovalent iron. Column B had a dry weight of 2273 g and a wet weight of 2507 g. The pore volume for column B was 208.9 mL. The porosity of both columns was 0.49. These porosity values are similar to those measured for zerovalent iron columns and field scale PRBs (*11*, *13*, *16*). Prior to transporting the columns to the field site, the columns were flushed with CO_2 gas for several hours to remove most atmospheric air. This gas was chosen because it is soluble in water, which facilitates saturation of the column with water. The influent and effluent tubes were then sealed for transport.

* Corresonding author phone: (519) 253-3000 ext. 4730; e-mail: weisener@uwindsor.ca.

† Current address: Great Lakes Institute for Environmental Research, University of Windsor, Windsor, Ontario, Canada N9B 3P4.

10.1021/es050092y CCC: $30.25
Published on Web 07/13/2005

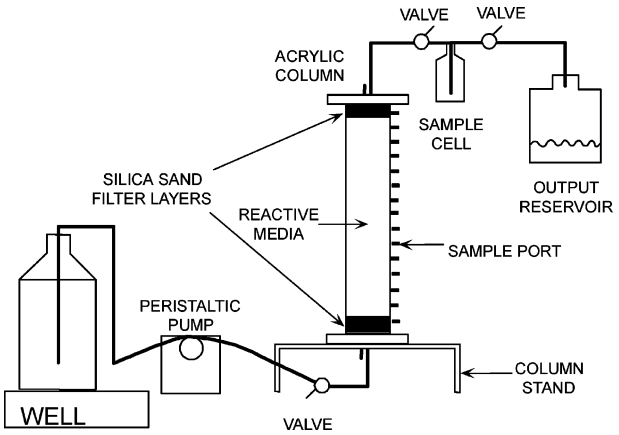

FIGURE 1. A schematic diagram of the column-testing apparatus. Groundwater from the well was pumped directly into the influent base plate of each column using a low-flow peristaltic pump. The effluent was discharged through the top plate of the column. The input samples were collected from the control valve in the influent line and the effluent samples collected from the sampling cell. Each column was 21.7 cm (0.72 ft) in length and 5 cm (2 in.) in diameter. Six lateral sampling ports were located along the length of the columns.

The column-test apparatus was housed in a mobile trailer positioned over a monitoring well. Each column had a dedicated low-flow peristaltic pump attached to a length of narrow-diameter (3.15 mm) Teflon tubing that extended directly into the well. An extension PVC pipe and socket-fitting couple was attached to the upper end of the monitoring well to minimize the potential for the introduction of surface runoff to the groundwater while the test was in progress. Groundwater sampled from the well was pumped directly into the influent base plates of each column using low-flow peristaltic pumps. Initially, the columns were filled with groundwater over a period of approximately an hour to displace all gas from the column and tubing. The columns were then temporarily disconnected from the pumps so that the saturated mass of each column could be measured.

Water Flow Characteristics. Flow to the columns was maintained uniformly over a 42 day period. The total volume of flow for the 42 day period through columns A and B was 19.54 and 83.14 L, respectively. This flow corresponded to 92.9 pore volumes of flow for column A and 398.0 pore volumes for column B. The pumping rates for the test were established to simulate 10 years of groundwater flow through a permeable barrier system in the high-flow column (column B) and approximately 2 years of flow through the low-flow column (column A). The target flow rates for the two columns were approximately 2 and 0.4 L day^{-1}, respectively. On average 0.465 L day^{-1}, or 2.2 pore volumes per day, of groundwater was introduced to column A and 1.98 L/day or 9.5 pore volumes per day was introduced to column B. The residence time of groundwater in columns A and B was 10.8 and 2.5 h, respectively.

Analytical Methods. Groundwater samples were collected from the sampling ports. A syringe was attached to each port so that it filled at the same rate as the introduced water to the column (approximately 10 and 100 mL/h for the low-flow and high-flow columns, respectively). The collected water was transferred to 40-mL glass volatile organic analysis (VOA) vials for mercury analysis and into plastic vials for the analysis of major anions, cations, and metals. The samples for analysis of dissolved cations and dissolved metals were acidified to pH < 2 with high-purity nitric acid. Samples for dissolved mercury determinations were preserved using ultrapure HCl acid to pH < 2. The samples for total and methyl mercury were shipped in ice-packed coolers to Frontier Geosciences, Seattle, WA. Alkalinity, Eh, and pH measurements were made immediately following the collection of the samples. Alkalinity was measured in a laboratory building adjacent to the test site using a Hach digital titrator (Titration Method 2320 B; American Public Health Association (APHA), 1992). Eh (Oxidation−Reduction Potential Method 2580 B; APHA, 1992) and pH (Electrometric Method 4500-H^+ B; APHA, 1992) measurements were made in the field trailer using Orion and Orion Ross electrodes, respectively, immediately after the sample had been collected in the syringe at the field site. Total mercury was determined using cold vapor-atomic fluorescence spectrometry (CV-AFS) by Frontier Geosciences. This method employs iodine-impregnated activated carbon traps. The carbon traps adsorb both the oxidized (Hg^{2+}) and elemental (Hg^0) forms of mercury, resulting in a total mercury determination. The carbon trap is divided into two zones. The first functions as the sample collection trap and the second serves as a field blank or breakthrough indicator. Methyl mercury analysis was also performed by Frontier Geosciences using aqueous-phase ethylation. Ethylation is performed using a complexing agent of sodium tetraethylborate. After formation of the complex, the methylmercury hydride and Hg^0 are preconcentrated using a carbon trap and are then separated chromatographically using an isothermal gas chromatograph, followed by cold vapor atomic fluorescence spectrometry (CH_3Hg; EPA Method 1630). Sulfate and other anions were analyzed using Ion Chromatography (IC; EPA Method 300.0).

Mineralogical Characterization of the Column Solids. Following completion of the field tests, the columns were transported to the University of Waterloo and stored in a cold room (4 °C) under sealed static conditions. Samples of reactive material from columns A and B were extracted from three representative sampling points (influent bottom, port 3, and effulent top) within an argon-purged glovebox to minimize oxidation. The samples were sealed in argon-purged glass vials for thin section preparation and examination using a LEO 1539 field emission secondary electron microscope. EDX analyses were obtained using an EDAX Pegasus 1200 integrated EDX/OIM. The cinnabar standard was provided by Natural Resources Canada, Ottawa, and was validated using XRD. The metacinnabar standard was obtained from Alfa Aesar Ward Hill USA.

XAFS Analysis. Hg L_{III}-edge μ-SXRF and μ-XAS measurements were performed at the Advanced Photon Source (APS), Argonne National Laboratory (Chicago, IL). Beamline 13-ID-C is equipped with Kirpatrick-Baez optical geometry to focus the monochromatic light obtained from a Si crystal monochromator down to 1−5 μm. The detector used at 13ID-C was a 13 element germanium detector with a 100-μm aluminum filter to prevent saturation of the detector from high Fe K-edge fluorescence. The scans were collected from 100−50 eV before the edge to 200−600 eV above the edge. All spectra were processed by subtracting the pre-edge and post-edge backgrounds and normalizing the step height to 1. XAFS data reduction and single-shell analysis was performed using the program IFEFFIT (*27*). The XAFS spectra were processed by averaging data scans collected, background removal to isolate the fine structure scattering component, and Fourier transformations of the scattering curve to obtain a radial structure function (RSF). The XAFS scattering curve was weighted by k^3 (k is the electron wave vector) during the background removal and prior to the Fourier transformation to enhance weak scattering oscillations. The XAFS spectra were Fourier-transformed using an unsmoothed window over the k range from 2 to 13 Å^{-1} to yield a RSF plot. A narrower k range (i.e., 2−8 Å^{-1}) was chosen for the analyzed column material due to low concentrations and to eliminate noisy data at the high end of the XAFS spectra. Coordination numbers were kept invariable in the

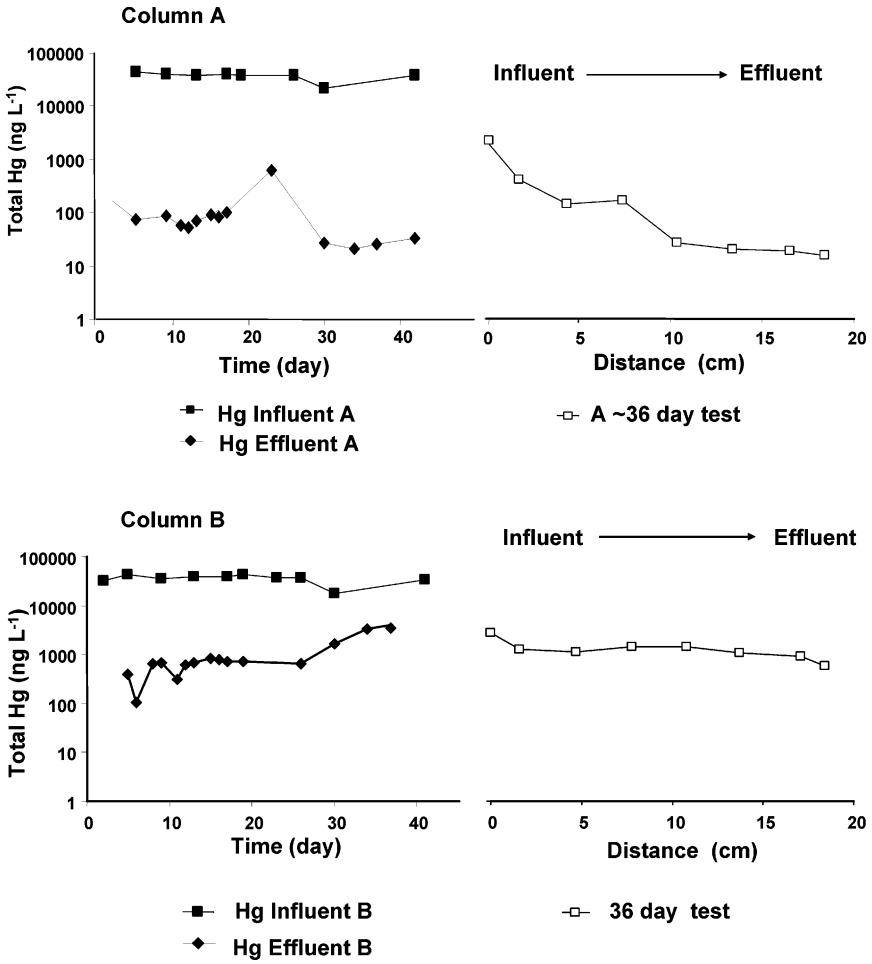

FIGURE 2. Comparisons of the total mercury concentrations as a function of time in the effluent and the influent groundwater in columns A and B over the 42-day period. The second plot shows the distribution profile of total mercury as a function of distance traveled up through the reactive media in columns A and B.

refinement for the first shell. Locations of the peaks in each RSF spectrum represent the distances between the absorber and successive shells of neighboring atoms; these are uncorrected for phase shift. Mineral standards used for obtaining XAFS fitting parameters were mercurous oxide, calomel, cinnabar ($HgS_{hexagonal}$), and metacinnabar (HgS_{cubic}).

Results and Discussion

Water Chemistry and Mercury Removal. The pH of the influent groundwater ranged from 7.8 to 9.5. The higher pH values in this range where observed during heavy rainfall periods during the course of the experiment. The influent groundwater was moderately reduced with the Eh ranging between 0 and 120 mV. The influent groundwater contained between 30 and 40 mg L^{-1} Cl, typically less than 1 mg L^{-1} NO_3, and 150−600 mg L^{-1} SO_4. Alkalinity ranged from 270 to 500 mg L^{-1} (expressed as $CaCO_3$). The groundwater also contained approximately 300 mg L^{-1} Na, between 5 and 70 mg L^{-1} Ca, and between 2 and 25 mg L^{-1} Mg. Iron was not detected (<0.05 mg L^{-1}) in any samples. The total mercury concentration ranged from 18 to 42.5 μg L^{-1}. Methyl mercury concentrations in the influent were below the detection limit. The pH of the effluent from column A ranged from 8.95 to 10, and was typically slightly higher than the pH of the influent groundwater measured on the same day. The Eh values of the effluent from column A were low, ranging from −45 to 75 mV. The Eh and alkalinity of the effluent was slightly lower than that of the influent groundwater. The alkalinity values were typically in the range from 100 to 435 mg L^{-1} (as $CaCO_3$). Chloride (25−40 mg L^{-1}) and sulfate (150−580 mg L^{-1}) concentrations were similar to those of the influent groundwater, but the concentration of nitrate in the effluent was consistently less than 0.2 mg L^{-1} (NO_3) and less than 0.07 mg L^{-1} for the final 4 weeks of testing. The concentration of Na in the effluent was similar to that in the influent (~300 mg L^{-1}), but the concentrations of both Ca and Mg were typically less than 5 mg L^{-1} and lower than those in the influent groundwater, suggesting possible precipitation in the column. The dissolved Fe concentration in the effluent from column A was below the detection limit of 0.05 mg L^{-1} in all samples. The total mercury concentration in the effluent from column A ranged from 0.168 to 0.021 μg L^{-1}. The data for the port profiling on day 36 suggest that the changes in chemical characteristics between the influent and effluent in column A evolved with distance through the zerovalent iron. A comparison of the total mercury concentrations as a function of time in the effluent and influent groundwater from columns A and B along with the distribution profile of total mercury as a function of distance through each column is shown in Figure 2.

The water chemistry of the effluent from column B was generally similar to that of column A with a few exceptions. The values of Eh, pH, Cl, and SO_4 concentrations were the same for both columns. However, slight differences were observed in the performance of column B when compared to column A. Changes in alkalinity between the influent and effluent were not apparent in column B. The effluent from column B also showed low concentrations of dissolved Fe (0.5 mg L^{-1}); dissolved Fe was detected on several sampling occasions and staining was observed at the top of the end

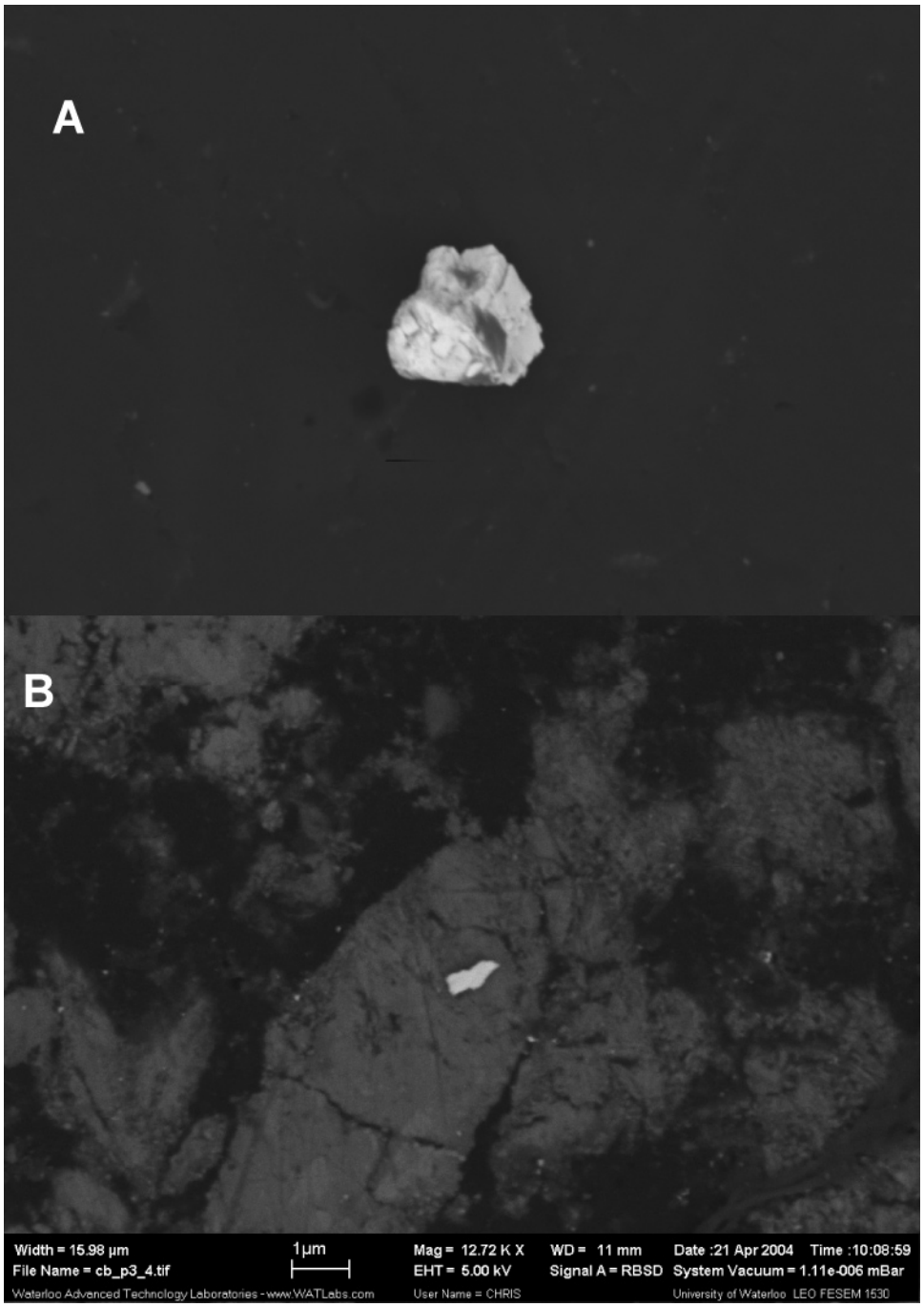

FIGURE 3. Mercuric sulfide precipitates observed as both granular liberated particles with pseudo cubic inclusions (A) and an enclosed HgS particle encapsulated in iron oxyhydroxides (B).

plate and effluent tubing toward the end of the experiment. This staining and the measurable concentrations of Fe in the effluent result from the release of dissolved Fe(II) coupled with the oxidation of Fe(0). The concentration of total mercury in the effluent from column B increased from less than 0.5 μg L^{-1} within the first week of testing to 4 μg L^{-1} on day 37. Figure 2 shows the total mercury concentrations with time in the effluent from column B, and also illustrates the distribution of total mercury with distance through the zerovalent iron. The potential for the zerovalent iron to remove mercury from the groundwater concentration to less than 1 μg L^{-1} was exceeded by the middle of the testing period at the higher flow rate.

Solid-Phase Precipitates Observed in Columns A and B. The removal of Hg, Ca, and Mg as groundwater moved through the columns suggests that precipitation or adsorption reactions are occurring (i.e., formation of carbonates and mercury compounds within the columns). Column materials were collected from the inlet, middle, and outlet ports of columns A and B. Backscattered electron micrographs in conjunction with EDX chemical analysis identified small clusters of $CaCO_3$ crystals associated with the zerovalent iron particle from the inlet material in column A. The mass of carbonate precipitates, however, is small relative to the volume of water that has passed through the columns. Thin sections of the column material were prepared to examine the morphological characteristics and the composition of the mercury-bearing precipitates which accumulated in the test columns. Mercury sulfide precipitates that were observed in column A collected near the column inlet. There was no

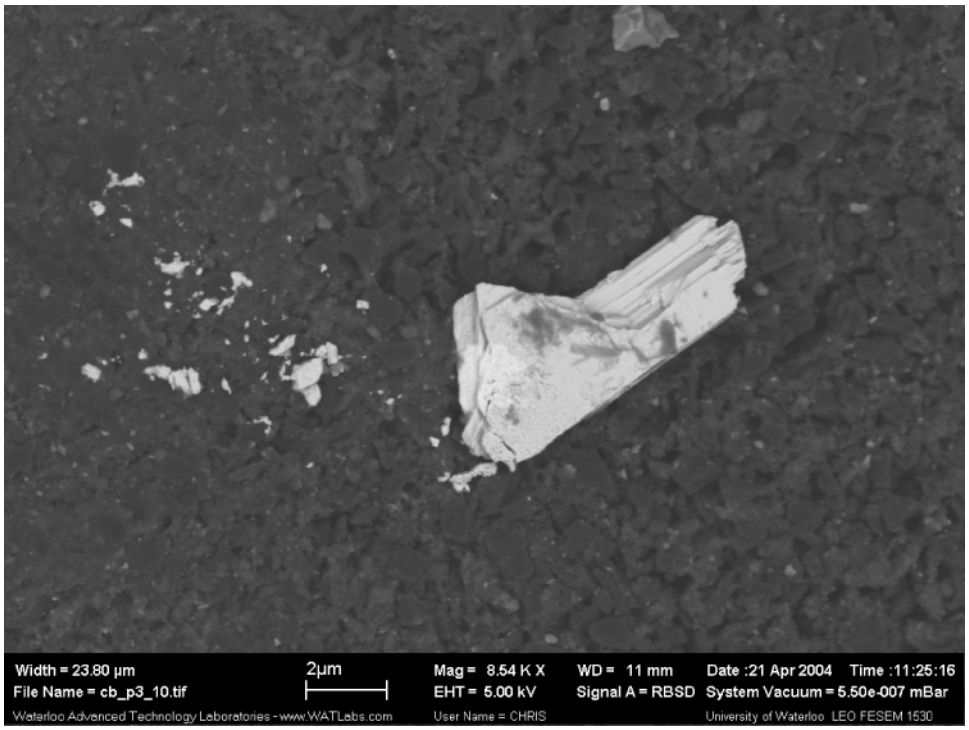

FIGURE 4. Mercuric sulfide precipitates shows well-defined crystal habit forming sheet like tabular grains.

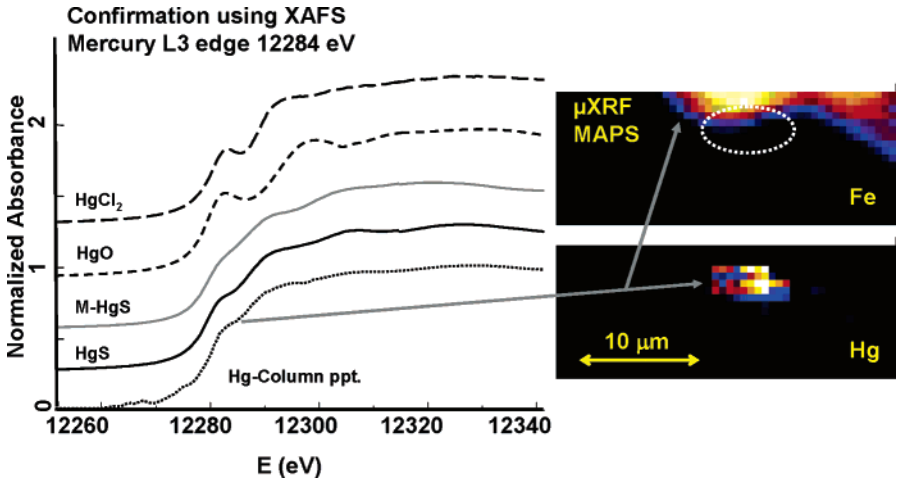

FIGURE 5. Figure shows a comparison of the Hg L_3-edge XANES spectra collected from a μXRF mapped region for the representative standards and the collected material from column B.

evidence of any mercury sulfide precipitates in samples collected from the middle of the column or the effluent end of column A.

Aqueous profile sampling in the low-flow column suggests that most of the mercury removal had occurred within the lower half of the reactive zone. The mercury-bearing precipitates observed in column A are small individual ~1 × 2 μm grains confined to the inlet portion of the column. No direct physical association was observed between the granular iron and these mercury sulfide grains. In contrast, column B, simulating a 10-year exposure, showed the presence of mercury precipitates at both the inlet and the middle sample locations. No mercury precipitates were observed in the outlet sample location. The mercury sulfide grains isolated from column B were larger, ranging from individual grains of 2−5 μm, which occurred in clusters. In some areas grains were encased in iron oxyhydroxides (Figure 3). The larger grains appear to have tabular crystal habits (Figure 4). The SEM-EDX chemical composition of the analyzed mercury sulfide grains shows an average stoichiometry of $HgS_{0.85}$. All of the mercury-bearing grains analyzed are sulfur-deficient compared to the stoichiometry of 1:1 observed in cinnabar and metacinnabar. The presence of a mercury sulfide phase was confirmed by collecting μSXRF maps and μEXAFS analysis of the localized mercury precipitates from column B. A comparison of the μXANES spectra collected from the mercury precipitate shows a strong correlation with the cinnabar standards analyzed (Figure 5).

Hg XAFS. Figure 6 shows the Hg L_3-edge Fourier transform spectra of the analyzed mercury standards and the inlet sample collected from column B. Sample description and fit results are provided in Table 1. The XANES and the k^3 weighted χ function of the XAFS region and its Fourier transform indicate that the solid Hg phase observed has a structure similar to that of metacinnabar. The interatomic distances for Hg−S measured from the cinnabar and metacinnabar standards were 2.38 Å for cinnabar and 2.51 Å for metacinnabar. These values agree favorably with the theoretical values of 2.37 and 2.53 Å for these compounds (*28*).

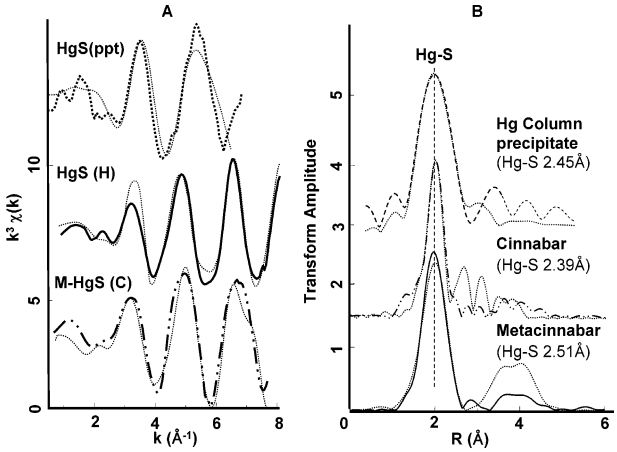

FIGURE 6. (A) shows the Hg L_3-edge Fourier transform spectra of the mercury standards and the inlet sample collected from column B. The XANES and the k^3 weighted χ function of the XAFS region and its Fourier transform indicate that the solid Hg phase observed has a structure similar to that of metacinnabar. (B) The interatomic distances for Hg−S measured from the cinnabar and metacinnabar standards were 2.39 Å for cinnabar and 2.51 Å for metacinnabar. These bond distances agree favorably with the theoretical bond distances of 2.37 and 2.53 Å for the first shell of these compounds. Only the first shell representing Hg−S from the standards and column precipitate was fit.

TABLE 1. XAFS Analysis of HgS Standards and Column Precipitate

sample	scatterer	CN[a]	*R* [Å][b]	σ^2 [Å^2][c]	*R*-factor[d]
Cinnabar	S	2	2.38	0.003	5.2
Metacinnabar	S	4	2.51	0.003	6.3
column solid	S	3.5	2.45	0.004	12.3

[a] Coordination number. [b] Radial distance absorber−scatterer distance. [c] Debye−Waller factor. [d] Goodness of fit.

The first Hg−S shell from the column precipitate material was fit.

A summary of the XAFS fits for the column precipitate, cinnabar, and metacinnabar standards are shown in Table 1. Due to the low volume of sample analyzed in this case adequate XAFS signal was not achieved at higher k ranges. Adequate interpretation of the second and third shells was not possible. Despite this limitation, an average interatomic distance of 2.45 Å with 3.5 sulfur atoms for the Hg−S first shell was determined for the precipitates observed in column B. This interatomic distance suggests that the mercuric compound formed in column B has an interatomic distance that is intermediate between cinnabar and metacinnabar.

The development of metacinnabar-like phases in sulfidic solutions has been observed by Charnock et al. (*28*). During the initial stages of precipitation, mercury sulfide phase develops with low coordination linear structures, which evolves to a 4-fold coordinated mercury-sulfide compound over time (*28*). The formation of these mercury sulfide phases may be partly controlled by the structure of mercury-sulfide complexes in solution (i.e., aqueous HgS_2^{2-} polysulfide complexes) at pH values greater than 8 under anoxic conditions (*28*, *29*). Under these conditions the mercury phase evolves very quickly to form clusters which exhibit mercury coordination closer to four with the mercuric sulfide phase showing characteristics indicative of cubic metacinnabar (*28*). The mercuric sulfide precipitate observed in column B has a Hg−S interatomic distance of 2.45 Å, which is shorter than that observed in metacinncabar. The column B precipitate seems to be an intermediate between cinnabar and a metacinnabar-like structure with low coordination.

Column Performance and Implication for Remediation. The removal of mercury and other electroactive metals by zerovalent iron occurs as a consequence of reductive precipitation or coprecipitation reactions on the grain surfaces of the iron (*11*, *14*). These reactions are limited kinetically, but generally occur at rates that are sufficiently rapid to remove contaminants at normal groundwater velocities. The flux of contaminants through zerovalent iron in the subsurface is influenced by the concentration of the contaminant and the groundwater velocity. The groundwater velocity in many hydrogeologic settings is of the order of 0.5 (15 cm) feet per day or less. The contaminant flux in the subsurface, therefore, can be modest and amenable to treatment using PRBs.

The results of the field column test suggest that removal of mercury by zerovalent iron was more successful under the low-flow conditions in comparison to the high-flow conditions for mercury removal. The flow corresponded to 93 pore volumes treated under the low-flow condition compared to 398 pore volumes for the high-flow condition. Total mercury in the effluent of the high-flow column was decreased to less than 0.5 μg/L during early operation when the influent contained 40 μg/L. The higher velocity was chosen to simulate 10 years of treatment. In contrast, the low-flow column reduced the total mercury concentration to less than 0.035 μg/L for a sustained period during the final 3 weeks of the testing period. The mercury-removal performance was inversely related to the flow rate through the columns. It is reasonable to suggest that improved mercury removal could be achieved with longer residence time of groundwater anticipated within the proposed zerovalent iron treatment zone in the field. Profile sampling in the low-flow column prior to the end of testing suggested that most of the mercury removal had occurred in the initial 50% of the zerovalent iron. The reduced performance of the high flow through the column toward the end of the 28 day sampling period is related to an upward migration of a front of ferric oxyhydroxide precipitates which were visible in column B and not as apparent in column A. A factor controlling the advancement of this front is the increased rate of ingress of the oxygenated groundwater entering column B. Figure 6b shows a HgS precipitate sampled from the middle portion of column B is encased in Fe-oxyhydroxide.

Another possible influence on the performance of the zerovalent iron was the lack of contrast between the Eh and pH characteristics of the influent groundwater and the pore water in the column. The monitoring data indicate a slight decrease in Eh conditions as groundwater enters and passes through the zerovalent iron, and an increase of less than 0.5 pH units. Strongly reducing conditions within the zerovalent iron as a consequence of its corrosion reaction with water were evident in the removal of much of the influent nitrate, possibly by its abiotic reduction to ammonia. Nitrate concentrations in the influent groundwater were generally less than a few milligrams per liter. The Eh conditions observed in the field columns, however, were more oxidizing than are typically observed in zerovalent iron barriers in the field. The lowest Eh observed in column A was approximately −234 and −154 mV in column B. Eh values observed in field installations of PRB systems are typically less than −500 mV (i.e., Elizabeth City) (*30*). These much reduced conditions occur as a result of the reduction of water to H_2 gas. However, this reaction is kinetically limited. The residence time of groundwater in the columns during the field test was too short to permit extensive reduction of water. It is anticipated that more reduced conditions would be observed in a field scale installation for mercury removal. The results of this study suggest that treatment of mercury using zerovalent iron may be enhanced by maintaining adequate residence time. The governing reaction observed for Hg removal in

these two field column experiments can be described through reductive precipitation of the Fe^0 surface media and sulfate present in the groundwater:

$$4Fe^0(s) + SO_4^{2-}(aq) + 10H^+ \Rightarrow H_2S(g) + 4Fe^{2+}(aq) + H_2O(l)$$

$$H_2S(g) \Rightarrow S^{2-}(aq) + 2H^+(aq)$$

$$Hg^{2+}(aq) + S^{2-}(aq) \Rightarrow HgS(s)$$

As a result, under alkaline conditions and moderate Eh values reductive precipitation of mercuric sulfides can occur, forming a stable metacinnabar-like phase.

Acknowledgments

This research was supported in part by NSERC CRC program. XAFS spectroscopy data were collected from Advanced Photon Source (APS), Argonne National Laboratory, University of Chicago, BM 13-ID-C; supported by the U. S. Department of Energy, Office of Science, Office of Basic Energy Sciences, under Contract No. W-31-109-Eng-38. Thanks are extended to Matt Newville for his valued assistance with XAFS analyses setup and technical consultation.

Literature Cited

(1) King, J. K.; Harmon, S. M.; Fu, T. T.; Gladden, J. B. Mercury removal, methylmercury formation, and sulfate-reducing bacteria profiles in wetland mesocosms. *Chemosphere* **2002**, *46*, 859−870.
(2) Domagalski, J. Mercury and methylmercury in water and sediment of the Sacramento River Basin, California. *Appl. Geochem.* **2001**, *16*, 1677−1691.
(3) Gray, J. E.; Theodorakos, P. M.; Bailey, E. A.; Turner, R. R. Distribution, speciation, and transport of mercury in stream-sediment, stream water, and fish collected near abandoned mercury mines in southwestern Alaska, U.S.A. *Sci. Total Environ.* **2000**, *260*, 21−33.
(4) Kim, C. S.; Brown, G. E.; Rytuba, J. J. Characterization and speciation of mercury-bearing mine wastes using X-ray absorption spectroscopy. *Sci. Total Environ.* **2000**, *261*, 157−168.
(5) Munthe, J.; Lyven, B.; Parkman, H.; Lee, Y.-H.; Iverfeldt, A.; Haraldsson, C.; Verta, M. P. Mobility and methylation of mercury in forest soils development of in-situ stable isotope tracer technique and initial results. *Water, Air, Soil Pollut.: Focus* **2001**, 385−393.
(6) Rytuba, J. Mercury mine drainage and processes that control its environmental impact. *Sci. Total Environ.* **2000**, *260*, 57−71.
(7) Sladek, C.; Gustin, M. S. Evaluation of sequential and selective extraction methods for determination of mercury speciation and mobility in mine waste. *Appl. Geochem.* **2003**, *18*, 567−576.
(8) Mason, R. P.; Reinfelder, J. R.; Morel, F. M. Uptake, Toxicity, and Trophic transfer of mercury in a coastal diatom. *Environ. Sci. Technol.* **1996**, *30*, 1835−1845.
(9) Mackay, D. M.; Cherry, J. A. Groundwater contamination: pump-and-treat remediation. *Environ. Sci. Technol.* **1989**, *23*, 630−636.
(10) Waybrant, K. R.; Ptacek, C. J.; Blowes, D. W. Treatment of mine drainage using permeable reactive barriers: column experiments. *Environ. Sci. Technol.* **2002**, *36*, 1349−1356.
(11) Blowes, D. W.; Ptacek, C. J.; Benner, S. G.; McRae, C. W. T.; Bennett, T. A.; Puls, R. W. J. Treatment of inorganic contaminants using permeable reactive barriers. *Contam. Hydrol.* **2000**, *45*, 123−137.
(12) Waybrant, K. R.; Blowes, D. W.; Ptacek, C. J. Selection of reactive mixtures for use in permeable reactive walls for treatment of mine drainage. *Environ. Sci. Technol.* **1998**, *32*, 1972−1979.
(13) Blowes, D. W.; Ptacek, C. J.; Jambor, J. L. *In situ* remediation of Cr(VI)-contaminated groundwater using permeable reactive walls: laboratory studies. *Environ. Sci. Technol.* **1997**, *31*, 3348−3357.
(14) Benner, S. G.; Blowes, D. W.; Ptacek, C. J. *Abstr. Pap. Am. Chem. Soc.* **1997**, *213*, 45-Envr.
(15) Benner, S. G.; Blowes, D. W.; Gould, W. D.; Herbert, R. B., Jr.; Ptacek, C. J. Geochemistry of a permeable reactive barrier for metals and acid mine drainage. *Environ. Sci. Technol.* **1999**, *33*, 2793−2799.
(16) Morrison, S. J.; Metzler, D. R.; Carpenter, C. E. Uranium precipitation in a permeable reactive barrier by progressive irreversible dissolution of zerovalent iron. *Environ. Sci. Technol.* **2001**, *35*, 385−390.
(17) Ludwig, R. D.; McGregor, R. G.; Blowes, D. W.; Benner, S. G.; Mountjoy, K. *Ground Water* **2002**, *40*, 59−66.
(18) Pratt, A. R.; Blowes, D. W.; Ptacek, C. J. Products of chromate reduction on proposed subsurface remediation material. *Environ. Sci. Technol.* **1997**, *31*, 2492−2498.
(19) Herbert, R. B.; Benner, S. G.; Blowes, D. W. Solid phase iron−sulfur geochemistry of a reactive barrier for treatment of mine drainage. *Appl. Geochem.* **2000**, *15*, 1331−1343.
(20) Weisener, C.; Gerson, A. Cu(II) adsorption mechanism on pyrite: an XAFS and XPS study. *Surf. Interface Anal.* **2000**, *30*, 454−458.
(21) Behra, P.; Bonnissel-Gissinger, P.; Alnot, M.; Revel, R.; Ehrhardt, J. J. XPS and XAS study of the sorption of Hg(II) onto pyrite. *Langmuir* **2001**, *17*, 3970−3979.
(22) Brown, G. E., Jr.; Calas, G.; Waychunas, G. A.; Petiau, J. In *Spectroscopic Methods in Mineralogy and Geology*; Reviews in Mineralogy; The Mineralogical Society of America: Washington, D.C., 1988; Vol. 18, pp 431−512.
(23) Manceau, A.; Tamura, N.; Celestre, R. S.; MacDowell, A. A.; Geoffroy, N.; Sposito, G.; Padmore, H. A. Molecular-scale speciation of Zn and Ni in soil ferromanganese nodules from loess soils of the mississippi basin. *Environ. Sci. Technol.* **2003**, *37*, 75−80.
(24) Weisener, C. G. In *Environmental Aspects of Mine Waste*; Jambor, J. L., D. W., B., Ritchie, A. I. M., Eds.; Mineralogical Association of Canada: Vancouver, 2003; Vol. 31, pp 181−202.
(25) Fenter, P. A.; Rivers, M. L.; Sturchio, N. C.; Sutton, S. R. In *Applications of synchrotron radiation in low-temperature geochemistry and environmental science*; The Mineralogical Society of America: Washington, D.C., 2002; Vol. 49, pp 1−50.
(26) Sham T. K. In *Synchrotron radiation earth, environmental and mineral sciences applications*; Henderson, G. S., Baker, D. R., Eds; Mineralogical Association of Canada: Ottawa, 2002; Vol. 30, pp 1−41.
(27) Newville, M. *J. Synchrotron Radiat.* **2001**, *8*, 322−324.
(28) Charnock, J. M.; Moyes, L. N.; Pattrick, R. A. D.; Mosselmans, J. F. W.; Vaughan, D. J.; Livens, F. R. The structural evolution of mercury sulfide precipitate: an XAS and XRD study. *Am. Mineral.* **2003**, *88*, 1197−1203.
(29) Barnes, H. L. Solubilities of ore minerals. In *Geochemistry of Hydrothermal Ore Deposits*; Wiley: London, 1979; pp 404−460.
(30) Puls, R. W.; Blowes, D. W.; Gillham, R. W. Long-term performance monitoring for a permeable reactive barrier at the US Coast Guard Support Center, Elizabeth City, North Carolina. *J. Hazard. Mater.* **1999**, *68* (1−2), 109−124.

Received for review January 14, 2005. Revised manuscript received May 11, 2005. Accepted June 7, 2005.

ES050092Y